Deposition of Submicron Charged Spherical Particles in the Trachea of the Human Airways.

Department of Engineering Sciences and Mathematics
Division of Fluid and Experimental Mechanics
Luleå University of Technology
*Corresponding author: S-97187 Luleå, Sweden, hake@ltu.se

Abstract: This paper presents a numerical study of the deposition of submicron charged spherical particles caused by convection, Brownian and turbulent diffusion in a pipe with a smooth wall and with a cartilaginous ring wall structure. The model is supposed to describe deposition of charged particles in generation 0 (trachea) of the human lung. The upper airways of the human lung are characterized by a certain wall structure called cartilaginous rings (fig.1) which are believed to increase the particle deposition when compared to an airway with a smooth wall. The problem is defined by solving the fluid flow problem with the aid of a low-Reynolds number k-epsilon model combined with a diffusion equation for the Brownian motion and Poissons equation for the electrostatic field. The electrostatic field is generated by the space-charge density of the particles. Results are presented for generation 0, the trachea of the human airways. Deposition results using Comsol multiphysics are compared with an analytic solution for the case of a fully-developed turbulent flow in an airway with a smooth wall.

Keywords: Charged nanoparticles, Brownian and turbulent diffusion, Electrostatics, Deposition, Human respiratory airways.

1. Introduction

Studies on particle transport of submicron particles are of high importance in the analysis of particle deposition in the respiratory airways, both for assessing health effects of inhaled toxic matter and for evaluating the efficacy of drug delivery with pharmaceutical aerosols.

Especially the nowadays so popular particles of nanometer size for the developing of new improved stronger materials and other fascinating technical applications are here of particular interest

In this paper we analyze how submicron particles (diameter<1μm) are deposited in the upper airways of the upper human lung airways and especially we consider the effects caused by charged spherical particles. We also include a wall structure called cartilaginous rings, located in the upper airways of the lung. In previous work (Åkerstedt(2010)[1],(2011)[2]) we have considered the lower airways (generation>4) of the human lung in which the flow is laminar. In the present paper we consider the corresponding problem for the upper airways, in particular the uppermost airway, the trachea (generation 0) in which the flow is usually turbulent.

To find the transport and deposition in a given flow geometry there are essentially two methods. A Lagrangian approach and an Eulerian approach. In the first method the motion of the individual particles in the flow field are tracked. For the laminar case the flow is generated by the Navier-Stokes equations while for the case of turbulent flow some turbulence model is adopted. The concept is then to launch a large number N of particles, derive their individual motion and compute particle deposition statistics from the fraction that hits a wall (Högberg et al.[3]). To get statistical measures of the deposition a large number of particles (N) need to be simulated with an error of the order $O(N^{-1/2})$ This Lagrangian approach is complicated if we for instance wish to find the electric field and force field from a concentration of charged particles. Since we consider the effect of a distribution of charged particles, the Eulerian method is chosen. The concentration is then governed by a convective diffusion equation including effects from Brownian motion D and migration in electric field. To include effects from a turbulent flow, turbulent diffusion D_t is added. For particles of size smaller than about 1μm, diffusion is the only effect from the turbulence. For larger particles, however, there is also an effect from turbophoresis (Guha(1997)[4]), which is a far more difficult problem to model, since anisotropic effects then become important, and thus cannot be modeled by for instance the simple turbulent k-ε model considered in the present paper.

2. Governing equations

The morphology of the respiratory airways of the human lung is represented by a bifurcating system of pipes where each pipe belongs to a certain generation. The uppermost airway (generation0) is a single pipe called trachea. The upper airways have a certain wall structure called cartilaginous rings, located in the upper airways of the lung see figure 1. In this paper we only consider results for this single pipe, the trachea.

For the analysis we assume a pipe with axial symmetry. The main flow is then in the *x*-direction and *r* is the coordinate in the radial direction. Since the flow in trachea is turbulent with a typical Reynolds number ranging from 2000 to 10000 we apply a low-Reynolds number incompressible k-ε model for the flow.

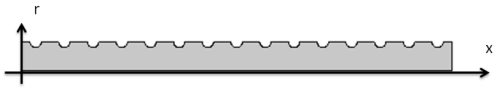

Figure 1. Axisymmetric pipe geometry with a cartilaginous ring wall structure. Radius of Trachea a=0.008[m] length 0.096[m]. Amplitude of rings 0.0008[m].

The equations for the fluid flow are then

$$\rho(\bar{\mathbf{u}}\cdot\nabla)\bar{\mathbf{u}} = \nabla\cdot(-\bar{p}\mathbf{I} + (\mu+\mu_t)(\nabla\bar{\mathbf{u}} + (\nabla\bar{\mathbf{u}})^T) - \frac{2}{3}\rho k\mathbf{I})$$

$$\nabla\cdot\bar{\mathbf{u}} = 0$$

$$\rho(\bar{\mathbf{u}}\cdot\nabla)k = 2\mu_t\nabla\bar{\mathbf{u}}\cdot\nabla\bar{\mathbf{u}} - \mu\nabla\bar{\mathbf{u}}\cdot(\nabla\bar{\mathbf{u}})^T + \nabla\cdot((\mu+\frac{\mu_t}{\sigma_k})\nabla k)$$

$$\rho(\bar{\mathbf{u}}\cdot\nabla)\varepsilon = C_{\varepsilon 1}\frac{\varepsilon}{k}2\mu_t\nabla\bar{\mathbf{u}}\cdot\nabla\bar{\mathbf{u}} - C_{\varepsilon 2}\frac{\varepsilon}{k}\rho\nu\nabla\bar{\mathbf{u}}\cdot(\nabla\bar{\mathbf{u}})^T +$$

$$+\nabla\cdot((\mu+\frac{\mu_t}{\sigma_\varepsilon})\nabla\varepsilon) - f_\varepsilon C_{\varepsilon 2}\rho\frac{\varepsilon^2}{k}$$

$$\mu_t = \rho f_\mu C_\mu \frac{k^2}{\varepsilon} \qquad (2.1)$$

with standard k-epsilon values for the constants and where f_ε and f_μ are the low-Reynolds number corrections.

The convective-diffusion equation including effects from a concentration *c* of charged particles with charge *q* and the electrostatic potential ϕ is of the form

$$(\bar{\mathbf{u}}\cdot\nabla)c - \frac{qD}{\kappa T}(\nabla c\cdot\nabla\phi) + \frac{q^2D}{\varepsilon_0\kappa T}c^2 - \nabla\cdot((D+D_t)\nabla c) = 0 \qquad (2.2)$$

Here D is the Brownian diffusion coefficient given by

$$D = \frac{\kappa T\, Cu}{3\pi\mu d}$$

$$Cu = 1 + \frac{\lambda}{d}(2.34 + 1.05\exp(-0.39\frac{d}{\lambda}))$$

where *Cu* is the Cunningham factor which is a correction factor needed to bridge the gap between the continuum limit and the free molecular limit for the flow past a spherical particle. λ is the collision mean free path and *d* is the particle diameter, κ is Boltzmann's constant, *T* is the absolute temperature and μ is the dynamic viscosity of the air.

The turbulent diffusion coefficient is related to the turbulent viscosity as

$$D_t = \frac{\mu_t}{\rho}$$

In the presentation of the results it is also convenient to introduce the dimensionless number α

$$\alpha = \frac{1}{4}\frac{c_0 q^2 a^2}{\varepsilon_0\kappa T}$$

The electrostatic potential is given by Poisson's equation

$$\nabla^2\phi = -\frac{qc}{\varepsilon_0} \qquad (2.3)$$

which is the equation providing the connection between the charge distribution and the electrostatic potential.

3. Use of COMSOL Multiphysics

The set of equations (2.1-2.3) are solved together using Comsol Multiphysics 4.3. The different physics interfaces used are the low-Reynolds number k-ε model for turbulent flow, Transport of diluted species and Electrostatics.

At the inlet x=0 a uniform velocity is chosen and at x=L fluid flow outlet conditions are applied. On the x-axis axial symmetry is chosen.
For the transport of diluted species interface the concentration at the inlet is uniform $c = c_0$. The boundary condition of the absorbing wall is $c = 0$ and at the outlet convective flux is chosen. For the electrostatics interface, zero charge is chosen at the inlet and outlet. Since the wall of the respiratory airways consists of a so called mucus-layer including mainly water, the wall is treated as a good conductor so the wall potential is chosen as zero. For the meshing settings a fine physics-controlled mesh is applied.

4. Validation of Comsol model with theory for a smooth pipe

To validate the results using Comsol Multiphysics we first consider some approximate analytical results of the deposition of charged particles in a fully-developed turbulent flow in a simple smooth pipe.

We assume that the concentration is uniform equal to c_0 except in a thin layer close to the boundary. An approximate solution of Poisson's equation is then simply

$$\phi = \frac{c_0 q}{4\varepsilon_0}(a^2 - r^2) \qquad (4.1)$$

It is convenient to introduce dimensionless quantities. The dimensionless distance from the wall is introduced as

$$y^+ = Re_*(1 - \frac{r}{a})$$

where the Reynolds number Re_* based upon the friction velocity is defined as

$$Re_* = \frac{a u_*}{\nu}.$$

Here u_* is the friction velocity given by

$$u_* = \sqrt{\frac{\tau_w}{\rho}},$$

where τ_w is the wall shear stress.

For the fully developed case the convective-diffusion equation (2.2) in the thin layer approximation then becomes

$$\alpha \frac{D^+ c_0}{Re_*}\frac{\partial c}{\partial y^+} + \frac{\partial}{\partial y^+}(D^+ + D_t^+)\frac{\partial c}{\partial y^+} = 0 \qquad (4.2)$$

where $D^+ = \frac{D}{\nu}$ and $D_t^+ = \frac{D_t}{\nu}$. Integrating this equation gives

$$\frac{\alpha D^+}{Re*} c_0\, c + (D^+ + D_t^+)\frac{\partial c}{\partial y^+} = c_0\, V_{dep}^+$$

where $V_{dep}^+ = \frac{V_{dep}}{u_*}$ is the dimensionless deposition velocity. The solution is

$$c(y^+) = c_0 \frac{Re_* V_{dep}^+}{\alpha D^+}(1 - \exp(-\frac{\alpha D^+}{Re_*} Z(y^+))) \qquad (4.3)$$

where $Z(y^+) = \int_0^{y^+} \frac{dY}{D^+ + D_t^+(Y)}$

The deposition velocity can be obtained by taking the limit $y^+ \to \infty$

$$V_{dep}^+ = \frac{\alpha D^+}{Re*(1 - \exp(-\frac{\alpha D^+}{Re*} Z(\infty)))}. \qquad (4.4)$$

It is seen that the deposition velocity is determined once a model for the eddy diffusivity D_t^+ is known. The largest contribution to the integral in (4.4) however comes from the region near the wall and therefore it is sufficient to know its behavior for small y^+. The small y^+ behavior of the eddy diffusivity is well known from experiments as

$$D_t^+ = A\, y^{+3} + \ldots = 6.1 \cdot 10^{-4}\, y^{+3} + \ldots \qquad (4.5)$$

The integral in(4.4) then becomes

$$Z(\infty) = \frac{2\sqrt{3}\,\pi}{9\, A^{1/3} D^{+2/3}} \qquad (4.6)$$

The result for the deposition velocity is then

$$V_{dep}^{+} = \frac{\alpha D^{+}}{Re_{*}(1-\exp(-\frac{\alpha D^{+1/3} 2\sqrt{3}\pi}{9 \cdot Re_{*} A^{1/3}}))} \cdot \tag{4.7}$$

In the limit of zero charge $\alpha \to 0$ we find

$$V_{dep}^{+} = \frac{9 \cdot D^{+2/3} A^{1/3}}{2\pi\sqrt{3}} \tag{4.8}$$

and hence in the limit of $\alpha \to \infty$ we find simply

$$V_{dep}^{+} = \frac{\alpha D^{+}}{Re_{*}} \tag{4.9}$$

Next the analytical results are to be compared with the result from Comsol Multiphysics.
The calculation of the deposition velocity using Comsol Multiphysics is done as follows. The pipe is chosen sufficiently long so that the flow becomes fully developed. A length of about 80 times the radius is sufficient. The convective particle flux *chds.ncflux* is then integrated at two close x-positions, x_1 and x_2 ,in the fully developed region. The deposition velocity is then calculated from

$$V_{dep}^{comsol} = \frac{\int_0^a (chds.ncflux_2 - chds.ncflux_1) 2\pi r dr}{(x_2 - x_1) \cdot 2\pi a}$$

For the comparison we chose a Reynolds-number $Re = U_{mean} 2 \cdot a / \nu = 4000$ and three different diameters of the particles, *d*=10nm, *d*=100nm and *d*=1000nm. To find the effect of the charged particles we vary the electrostatic parameter α

$$\alpha = \frac{1}{4} \frac{c_0 q^2 a^2}{\varepsilon_0 \kappa T}$$

As an example if the concentration of particles at inlet is $c_0 = 1 \cdot 10^{11} [1/m^3]$ and the charge of the particles is $q = 40 \cdot 1.6 \cdot 10^{-19} [C]$ the electrostatic parameter is $\alpha = 3460$.

In **figure2** the deposition velocity calculated from the theory and Comsol Multiphysics are compared.

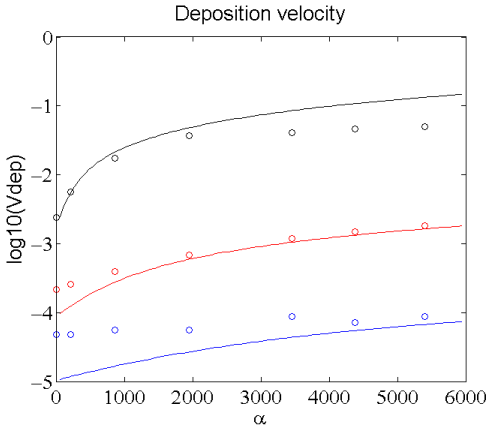

Figure 2. A comparison of deposition velocity calculated from theory (solid line) and calculated by Comsol Multiphysics (o). *d=10nm* (black), *d=100nm* (red), *d=1000nm* (blue)

From **figure 2** we note that there is some disagreement between theory and simulation especially for large particles (*d*=1000nm). For smaller particles there is better agreement and for the particle size *d*=10nm there is quite good agreement for small α while for *d*=100nm the agreement is good for larger α.

The reason for the failure using Comsol can be deduced from the behavior of the eddy diffusivity in the near-wall region. The correct behavior is given by (4.5). In **figure3** we have a comparison of the behavior of the eddy diffusivity from theory and Comsol. We note that the correct power of 3 in theory is much larger than the corresponding power in Comsol which from the figure can be estimated to be about 0.6. Since the correct behavior of the eddy diffusivity in the near wall region is very important for the prediction of the correct deposition velocity this explains the difference

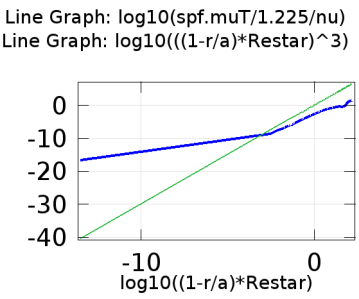

Figure 3. Behavior of eddy viscosity in the near wall region from theory (green) and using Comsol (blue).

between the results. The largest disagreement occurs for large particles, which can be understood by the magnitude of the Brownian diffusion D^+, which for large particles is very small. This together with the failure of the eddy diffusivity gives an error in deposition rate up to almost one order of magnitude.

For smaller particles for which Brownian diffusion dominates the sensitivity of the error in the eddy diffusivity is however not as important and for particles with diameter 100nm the agreement is quite good, at least for large α. For particles with diameter 10nm the agreement is quite good for small to medium α but not as good for large α. This disagreement for large α can be explained by the very thin boundary layers obtained in this limit, and may therefore be difficult to resolve numerically.

As a conclusion we can say that Comsol Multiphysics provides with reliable results at least for small particles less than 100nm and can therefore be applied also to the more complex geometry.

5. Particle deposition in trachea with a cartilaginous ring wall structure

Here we consider deposition results for the trachea as a pipe with a smooth wall and with the cartilaginous ring wall structure seen in **figure 1**. Since the most reliable results using Comsol for a smooth pipe are found for small particles we here only consider particles with diameter 10nm. The mean velocity is taken to be 4 [m/s] with a uniform distribution at inlet $x=0$.

Deposition rates are calculated using integration of the normal convective flux *chds.ncflux* across the inlet and outlet as

$$dep = \frac{\int_0^a (chds.ncflux_{out} - chds.ncflux_{in}) 2\pi r dr}{\int_0^a chds.ncflux_{in} 2\pi r dr} \tag{5.1}$$

The first case presented is for uncharged particles. In **figure 4** the streamlines of the velocity field and the variation in concentration

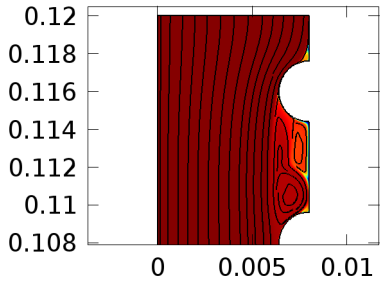

Figure 4. Flow in the neighborhood of the first ring. Streamline: Velocity field. Surface: Concentration. Lighter red means lower concentration.

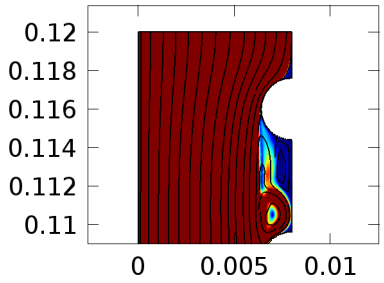

Figure 5. Streamline: Velocity field. Surface: Total particle flux magnitude. Dark red regions correspond to large flux and dark blue regions correspond to smaller flux.

is presented in the region before and after the first ring. Note that the flow separates after the first ring and also in a small region before the first ring. In the separated regions the concentration is lower than in the main stream. This does not mean that the deposition rate or particle flux in the separated regions is larger. The local deposition rate is determined from the local normal concentration gradients at the boundary. This can be seen from **figure 5** in which regions of dark red correspond to large particle flux and regions of dark blue to smaller particle flux.

Next the effect of charged particles is considered. As an example we consider the case of a concentration at inlet of $c_0 = 1 \cdot 10^{11}$ part/m^3, and that the charge of the particles is 40 times the elementary charge. This corresponds to a value of the electrostatic parameter α of 3459.

In **figure 6** the corresponding flow in the region behind the first ring is presented. In the separated region the concentration is somewhat smaller than for the case with uncharged particles. The electric field is therefore smaller in these regions compared with the region close to the rings. The particle flux due to electric mobility is therefore smaller and deposition rates in fact become smaller in these areas when compared to a smooth pipe. In the region near the rings the electric field is larger than for the case of smooth pipe. Total deposition is then a delicate balance of these effects.

In **figure 7** the total deposition is presented, calculated using (5.1) for a smooth pipe and a pipe with a cartilaginous ring structure. For uncharged particles $\alpha = 0$, the effect of the cartilaginous rings is to increase deposition while for larger values of α the situation is the opposite. Remarkably the effect of charged particles is the possibility to increase the amount of deposited particles from 1% for uncharged particles up to 25% for large α. These results should be useful in an optimal design of therapeutic aerosols.

6. Conclusions

The deposition of charged submicron spherical particles in the trachea of the human airways is investigated. Especially the effect of a cartilaginous ring wall structure is considered.

Since the fluid flow in trachea is in general turbulent a low-Reynolds number k-ε model is applied. The effect of Brownian and turbulent diffusion as well as migration of the charged particles in the self-consistent electric field is included.

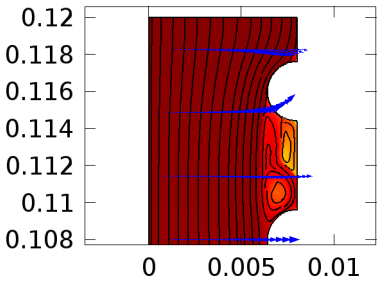

Figure 6. Streamline: Velocity field. Surface: Concentration. Arrow surface: Electric field

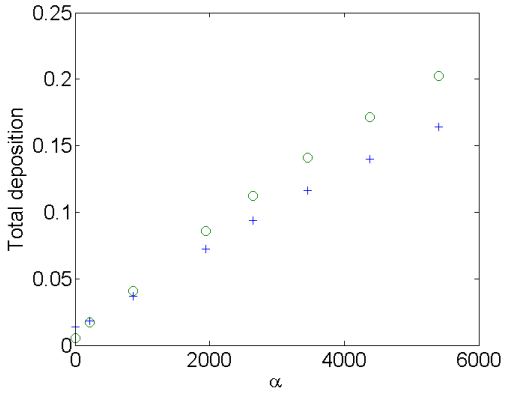

Figure 7. Total deposition as defined by (5.1). (o) smooth pipe. (+) pipe with cartilaginous ring structure.

The Comsol model is validated by comparing it with the theory for fully developed turbulent flow. The correct behavior of the eddy diffusivity in the near-wall region is shown to be crucial for a correct computation of the deposition. Deposition for three different diameters d=10nm, d=100nm and d=1000nm are considered. For the smaller particles d<100nm the agreement between theory is quite good. For the larger particles d=1000nm the agreement is poor. This failure of the Comsol model can be deduced from an incorrect behavior of eddy diffusivity in the near-wall region.

Since the Comsol model gives reliable results for small particles the model is used to estimate the deposition of 10nm particles in trachea with and without the cartilaginous ring wall structure. For uncharged particles the cartilaginous rings increase total deposition, while for a sufficiently large charge the effect is the opposite. In general charged particles enhance the total deposition with a possibility to increase particle deposition from 1% for uncharged particles up to 25% for charged particles. This result should be of importance in an optimal design of therapeutic aerosols.

7. References

1. Åkerstedt, H.O., The effect of cartilaginous rings on deposition by convection, Brownian diffusion and electrostatics. Comsol conference, Paris (2010)

2. Åkerstedt, H.O., Deposition of charged nano-particles in the human airways including effects from cartilaginous rings, *Natural Science*, Volume **3**, 884-888,(2011)

3. Högberg S.M., Åkerstedt H.O., Lundström T.S., Freund J., Respiratory deposition of fibers in the non-inertial regime: development and application of a semi-analytical model. *Aerosol Science and Technology.* **44,** 847-860(2010)

4. Guha, A., A unified Eulerian theory of turbulent deposition to smooth and rough surfaces, *Journal of Aerosol Science*, **28**, 1517-1537 (1997)

8. Acknowledgements

This work is sponsored by the Swedish Agency for Economic and Regional Growth and Centre for Biomedical Engineering and Physics.